Mon. Not. R. Astron. Soc. **000**, 000–000 (0000) Printed 1 February 2008 (MN LaTeX style file v1.4)

arXiv:astro-ph/9807110v3 23 Apr 1999

The Evolution of Rapid Burster Outbursts

R. Guerriero,[1] D. W. Fox,[1] J. Kommers,[1] W. H. G. Lewin,[1] R. Rutledge,[2] C. B. Moore,[3]
E. Morgan,[1] J. Van Paradijs,[4,5] M. Van der Klis,[5,6] L. Bildsten,[6] T. Dotani[7]
[1] *MIT Center for Space Research, 77 Massachusetts Ave #37-627, Cambridge, MA 02139-4307, USA*
[2] *Dept. of Astronomy, Caltech MC 220-47, Pasadena, CA 91125, USA*
[3] *Kapteyn Astronomical Institute, Postbus 800, 9700 AV Groningen, The Netherlands*
[4] *Univ. of Alabama in Huntsville, Huntsville, AL 35812, USA*
[5] *Astronomical Institute 'Anton Pannekoek' and Center for High-Energy Physics, Kruislaan 403, 1098 SJ Amsterdam, The Netherlands*
[6] *Depts. of Physics and Astronomy, University of California, Berkeley, Berkeley, CA 94720, USA*
[7] *Institute of Space and Astronautical Science, Sagamihara, Japan*

Received date. Accepted date.

ABSTRACT

We describe the evolutionary progression of an outburst of the Rapid Burster. Four outbursts have been observed with the *Rossi X-Ray Timing Explorer* between February 1996 and May 1998, and our observations are consistent with a standard evolution over the course of each. An outburst can be divided into two distinct phases: Phase I is dominated by type I bursts, with a strong persistent emission component; it lasts for 15–20 days. Phase II is characterized by type II bursts, which occur in a variety of patterns. The light curves of time-averaged luminosity for the outbursts show some evidence for reflares, similar to those seen in soft X-ray transients. The average recurrence time for Rapid Burster outbursts during this period has been 218 days, in contrast with an average ∼180 day recurrence period observed during 1976–1983.

Key words: X–rays: bursts – X–rays: stars – stars: individual: Rapid Burster – stars: variables: other

1 INTRODUCTION

The Rapid Burster (MXB 1730−335, or RB hereafter; Lewin et al. 1976), discovered in 1976, is a unique recurrent transient low-mass X-ray binary (LMXB). It is located at a distance of approximately 8 kpc (Ortolani, Bica, & Barbuy 1996) in the highly reddened globular cluster Liller 1 (Liller 1977). The RB is the only known LMXB to produce both type I and type II X-ray bursts (Hoffman, Marshall, & Lewin 1978a).

Although the RB has been studied for over twenty years, it is still not clear why the RB, and only the RB, emits both type I and type II X-ray bursts. Type I bursts are due to a thermonuclear flash of accreted material on the surface of a neutron star, and are characterized by a distinct spectral softening during burst decay. Of the ∼125 LMXBs known, at least 43 are type I burst sources (Van Paradijs 1995). Type II bursts are due to spasmodic accretion – the release of gravitational potential energy – presumably resulting from an accretion disk instability; the spectrum of these bursts shows little evolution during the burst. The duration of type II bursts can range from 680 seconds (the longest type II burst observed to date) down to 4 seconds. The behavior of type II bursts is like that of a relaxation oscillator: the type II burst fluence E is roughly proportional to the time interval, Δt, to the following burst (the 'E-Δt' relation: Lewin et al. 1976). The type II burst luminosities at burst maximum range from $\sim 4\times10^{37}$ to $\sim 3\times10^{38}$ erg s^{-1} (Lewin, Van Paradijs & Taam, 1993; henceforth LVT93). GRO J1744−28 is the only other LMXB known to emit repetitive type II bursts (Kouveliotou et al. 1996; Lewin et al. 1996a; Kommers et al. 1997). LVT93 provide a comprehensive review of type I and type II X-ray bursts and the Rapid Burster.

The pattern of type I and type II bursts, and the shape of the type II bursts themselves, have been observed to vary widely during a single outburst. At times, the RB emits only type I bursts with strong persistent emission (PE), behaving like a "normal" LMXB. At other times, type II bursts, occurring in a wide variety of forms and patterns, with or without substantial PE, are observed. When the RB is in a rapid bursting mode, it can emit thousands of rapid type II bursts per day, with little or no PE present. Short type II bursts typically exhibit a timescale-invariant profile, with multiple peaks ('ringing') during burst decay (Tawara et al. 1985). Bursts longer than about 35 seconds, on the other hand, are 'flat-topped' in shape (Lewin et al. 1976; Kunieda et al. 1984a; Stella et al. 1988a; Tan et al. 1991). An evolution from type I to type II bursting behavior was observed previously during the August 1983 outburst (Kunieda et al. 1984a; Barr et al. 1987)

© 0000 RAS

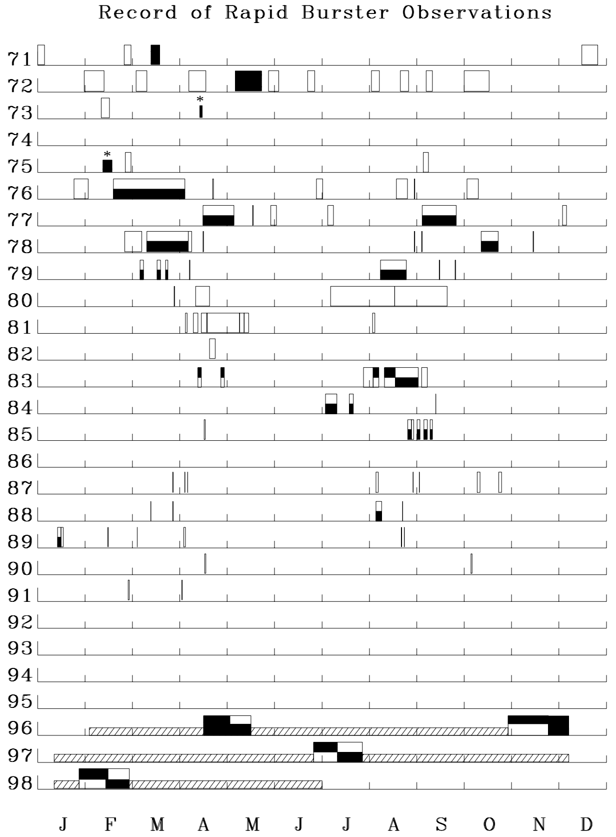

Figure 1. Record of observations of the Rapid Burster (1971-1998). Filled boxes indicate observations that occurred when the RB was active (a filled top half corresponds to Phase I, a filled bottom half to Phase II, and a completely filled box indicates that the phase could not be determined; see text). Open boxes indicate observations in which the RB was inactive. Single lines indicate observations of less than one day in which the RB was inactive. The observations marked with "*" indicate periods in which the source may have been active, but this is uncertain (White et al., 1978). Since February, 1996, the RB has been monitored for 11 months of the year with the *RXTE* ASM (slashed boxes). This figure is an extension of similar figures from Lewin and Joss (1983), and LVT93.

Quasi-periodic oscillations (QPO) in the 2–8 Hz frequency range are regularly seen in type II bursts from the RB, and occasionally in the PE (Tawara et al. 1982; Stella et al. 1988a,b; Dotani et al. 1990; Lubin et al. 1991; Rutledge et al. 1995). QPO are also present in many RB type II bursts in the form of the ringing observed during burst decay (LVT93). QPO have not been observed in any type I bursts from the RB. There are strong 0.04 Hz QPO present in the PE after some long type II bursts (Lubin et al. 1992b).

The outbursts of the Rapid Burster have long been known to recur every 6–8 months, based on observed outbursts (LVT93). Years at a time have passed without any positive detections; however, monitoring of the source has historically been sporadic (Figure 1). This changed in February 1996, when daily coverage of the RB (for 11 months of the year) began with the *Rossi X-ray Timing Explorer* (*RXTE*) All-Sky Monitor (ASM) (Levine et al. 1996).

Since then, we have observed four complete outbursts with *RXTE*. These outbursts have recurred at intervals of 200, 217, and 238 days. These outbursts show a nearly identical global evolutionary pattern: all four outbursts evolved, on the same timescale, from an initial phase dominated by type I bursts to a type II burst-dominated phase. This evolutionary progression may provide some insight into the unique behavior of the RB.

Rutledge et al. (1998) have observed a radio source at 4.5/8.4 GHz whose strength is correlated with the X-ray emission from the RB as measured by the *RXTE* ASM. They have proposed that this radio emission comes from the RB, even though the $\sim 1''$ position of the radio source lies well outside the 2σ error circle for the RB obtained with *Einstein* in 1984 (Grindlay et al. 1984; Moore et al. 1999).

We report here on our analysis of data taken with *RXTE* during the May 1996, November 1996, June 1997, and January 1998 outbursts of the Rapid Burster (Lewin et al. 1996b,c; Guerriero et al. 1997, 1998). In Section 2 we summarize our observations; in Section 3 we present the general evolution of a RB outburst; in Section 4 we compare our results to past observations of the RB with other satellites, and in Section 5 we give some possible interpretations of our findings.

2 OBSERVATIONS AND ANALYSIS

The RB was observed with *RXTE* on 31 separate occasions from May 3–13, 1996, November 6–17, 1996, June 26–July 30, 1997, and January 30–February 19, 1998 (Table 1). The total observing time during these periods was 7.5 ksec, 12.6 ksec, 35.0 ksec, and 44.8 ksec, respectively. Timing and spectral analyses were conducted with data collected with the Proportional Counter Array (PCA). The PCA consists of five identical xenon/methane proportional counters with a total effective area of approximately 6500 cm^2; it is sensitive to X-rays in the range 2–60 keV, and is capable of tagging relative event arrivals down to 1 μs (Zhang et al. 1993). Our observations used individually described, event-encoded data with a time resolution of 122 μs and 64 energy channels. The two standard data modes, providing $\frac{1}{8}$ s timing data and 16 s/129 energy channel data, were also available throughout.

The RB has been monitored almost continuously (except for $\sim$1 month per year when the source lies too close to the Sun) by the *RXTE* ASM since February 1996. The ASM consists of three identical Scanning Shadow Cameras (SSCs) mounted on a rotating assembly. Each SSC contains a position-sensitive proportional counter, which views the sky through a coded mask. The ASM is sensitive to X-rays in the range 2–10 keV. ASM data is taken in a series of 90 second "dwells", with any randomly selected source being scanned typically 5–10 times per day (Levine et al. 1996).

During the May 1996 outburst, the RB was observed with the PCA on three occasions near the end of the outburst (days 21–31 of the outburst) (Lewin et al. 1996b). On May 3 and May 7, 23 type II bursts of duration 8–17 seconds were observed. Bursts occurred every 80–100 seconds on May 3, and every 300–600 seconds on May 7. On May 13, no bursts were observed.

The RB was again observed with the PCA in November 1996, on days 8–19 of the outburst (Lewin et al. 1996c). One

Table 1. *RXTE* Observations of the Rapid Burster from 1996–1998. Day of outburst is calculated by considering the first $>3\sigma$ detection in the ASM to begin "day 1". Counts refer to the *RXTE* PCA (1 count $s^{-1} \simeq 3\times10^{-12}$ erg cm^{-2} s^{-1}; 2–20 keV). Type I burst durations were calculated by considering the end of the burst to be the point at which the excess burst flux returned to 10 per cent of its peak value. The count rates for all bursts and persistent emission during offset pointings have been corrected for aspect (factor of 2.5 for the RB).

Obs Start (UT)		Day of Outburst	Obs Duration (ksec)	Bursts Number Type I		Bursts Number Type II	Bursts Duration (s)	Average RB PE Level (cts s^{-1})
1996 May 03	15:25	21	1.5	0	+	15	9–16	400
07	15:37	25	3.0	0	+	8	8–17	250
13	12:19	31	3.0	0	+	0	n/a	180
1996 Nov 06	19:39	8	2.6	1	+	0	250	2270
09	00:31	11	2.7	1	+	0	200	1840
10	16:34	12	3.0	0	+	0	n/a	1370
11	21:23	13	1.8	1	+	0	30	1590
17	00:41	19	2.5	0	+	0	n/a	1090
1997 Jun 26	04:36	2	1.6	3	+	0	50–60	4630
26	08:01	2	2.1	4	+	0	100–200	4630
27	17:45	3	3.0	2*	+	0	150	4750
29	06:26	5	2.0	1	+	0	250	3320
29	17:53	5	2.6	2	+	0	150–180	3320
Jul 02	02:59	8	1.4	0	+	0	n/a	2400†
03	02:59	9	1.3	0	+	0	n/a	2400†
07	13:00	13	2.5	1	+	0	130–150	1200†
10	12:58	16	3.2	1*	+	0	70–100	1100†
13	11:09	19	3.6	1	+	2	Type I: 120 Type II: 180–420+	700
17	04:46	23	3.6	0	+	37	12–28	450
20	06:30	26	3.8	0	+	71	6–12	220
24	01:52	30	3.8	0	+	7	16–20	220
29	06:53	35	2.8	0	+	1	12	230
30	03:43	36	1.5	0	+	0	10–20	230
1998 Jan 30	17:12	3	6.5	5*	+	0	80–230	4000
31	22:57	4	3.5	2	+	0	180–220	2820
Feb 02	16:27	6	6.1	2	+	0	220–240	2370
04	19:48	8	3.5	1	+	0	240	2100
07	18:22	11	6.2	2	+	0	160–170	1030
10	21:26	14	6.6	1	+	0	170	1040
16	13:59	20	6.2	2	+	234	Type I: 40–50 Type II: 8–40	240
19	11:53	23	8.1	1	+	91	Type I: 50 Type II: 10–30	250

* One of these bursts was observed during a slew.

† Count rates are estimated; no offset pointing performed during these observations.

type I burst was observed during each of the observations on November 6, 9 and 11. The RB had an average persistent emission (PE) level on those three occasions of 2270 cts s^{-1}, 1840 cts s^{-1}, and 1590 cts s^{-1}, respectively. No bursts were observed on November 10 and 17. No PCA observations were possible after November 17, due to the *RXTE* Sun-angle constraint.

In June and July of 1997, the RB was observed at regular intervals throughout an entire outburst for the first time (Guerriero et al. 1997). Type I bursts were observed on days 2–17 of the outburst. On July 13, two "flat-topped" type II bursts of long duration (120 and >420 seconds, respectively) were observed. Rapid type II bursts were then observed until day 36 of the outburst, when the outburst ended (July 30). The PE level declined steadily throughout the outburst.

A second complete outburst was observed in January and February 1998 (Guerriero et al. 1998). Observations with the PCA began on day 3 of the outburst, and type I bursts were seen exclusively through day 14. On February 16, day 20 of the outburst, the RB was in a mode characterized by many rapid type II bursts, followed by a larger type II burst. This mode is identical to the mode in which the RB was discovered (Lewin et al. 1976). Rapid, regular type II bursting continued on February 19, the final observation of the outburst.

We have performed a spectral analysis to determine the conversion from count rates to fluxes and to draw some rudimentary conclusions about the X-ray emitting regions. We emphasize that the model we present is probably not uniquely indicated by the data. No single-component models provided acceptable fits to the data (minimum reduced chi-squared values, for 51 degrees of freedom, are $\chi^2_\nu \sim 3$ for type I bursts, 10 for type II bursts, and 170 for the PE). Two- and three-component models that we considered incorporated blackbody, disk blackbody, thermal bremsstrahlung, Comptonization, and power law spectral components. The best fitting models combined a power law with two blackbody components, resulting in $\chi^2_\nu = 0.8$–1.4. A simple two-component blackbody model, without a power law component, also provided statistically acceptable fits to most of the type I bursts, but for many type II bursts and the PE this model was not acceptable ($\chi^2_\nu = 6.8$ in some cases). The addition of a power law component improved the fits in these cases. None of the other models that we investigated provided statistically acceptable fits to the data.

Best-fit temperatures of the two blackbody components were 1.1–1.5 keV and 0.25–0.40 keV, respectively. Although the temperature of the hotter component in the type I bursts varied from burst to burst, it cooled by ∼0.2 keV over the course of the type I burst in nearly every case (see Section 3.1). The temperature of the cooler component remained relatively constant during type I bursts. The luminosity of the hotter component was ∼15 per cent that of the cooler component (2.5–20 keV), in the bursts and in the PE. When it was necessary to include a power law component in the model, the values for the photon index of the power law ranged from 1.9–4.0, and luminosities ranged from 1–2 per cent of the cooler component (2.5–20 keV). Most of the type II bursts and PE required a power law component in the spectral model to obtain an acceptable fit to the data. The neutral hydrogen column density for our models was fixed at 2×10^{22} cm^{-2}, as determined from *EXOSAT* observations (Tan et al. 1991); we did not find the low-energy spectral response of the PCA sufficient, in these observations, to constrain the column density independent of the other spectral parameters.

One possible physical picture suggested by this model is of a system with three X-ray emitting regions: the neutron star surface (∼1 keV blackbody), the accretion disk (∼0.3 keV blackbody), and a Comptonizing cloud of hot electrons (responsible for the power law component, when present). The cooling of the hotter blackbody component during type I bursts is consistent with a cooling neutron star surface (LVT93). In contrast, the roughly constant temperatures of the two blackbody components throughout the type II bursts suggest emitting regions that vary in size during the burst (normalizations of both components vary with the X-ray flux). We derive blackbody radii for the hotter component during the type I bursts of 9±2 to 14±2 d_8 km, depending on the burst, where d_8 is defined as $D/8$ kpc and D is the distance to the RB. During type I bursts the cooler component has a blackbody emitting area of 0.7±0.3 to 2.3±1.0 $\times10^6$ d_8^2 km^2.

For the type II bursts, we derive blackbody radii at the peak of the bursts of 5.0±1.0 to 10±1.5 d_8 km, depending on the burst, for the hotter component, and blackbody emitting areas of 0.5±0.3 to 2.1±0.9 $\times10^6$ d_8^2 km^2 for the cooler component. The normalizations of both components vary with total X-ray flux during the bursts.

For the persistent emission spectra, we derive blackbody radii for the hotter component of 10±2 to 13±2 d_8 km and blackbody emitting areas of 0.9±0.4 to 2.5±0.8 $\times10^6$ d_8^2 km^2 for the cooler component. The normalizations of both components decrease over the course of the outburst as the total X-ray flux decreases.

There are known problems with interpreting blackbody X-ray spectral fits in such a literal fashion (LVT93). One problem discussed in LVT93 is that the observed X-ray color temperature and the effective temperature (that is, the temperature if the source were a true Planckian emitter) can differ by as much as a factor of ∼1.5. In the present case, this could lead to blackbody radii $1.5^2 \sim 2$ times larger than the values we have quoted.

Bursts were classified as type I or type II, in part, by performing spectral fits on the "excess" (PE-subtracted) burst counts. This is not a perfectly straightforward procedure (Van Paradijs & Lewin 1985); however, while both type I and type II bursts can show some spectral evolution during the burst, the spectral softening during the decay is much more pronounced in a type I burst (cf. Figure 4). The burst profile of a type I burst, with a sharp rise and a roughly exponential decay, is also substantially different from that of a type II burst (except when the PE is near its peak level, when burst profiles alone are not sufficient to distinguish the two types). Together with the spectral fits, then, the burst profiles were used to classify bursts as either type I or type II.

The bright LMXB 4U 1728−34 lies only 0.5° from the RB and is in the field of view of the PCA when the RB is in the center of the field of view. To determine the contribution of this source, the satellite pointing was offset by 0.5° away from 4U 1728−34 for the last third of each observation. This procedure allowed us to estimate the number of counts arriving from each source, but reduced our count rate from the RB by about a factor of 2.5 for the offset phase of each observation. Additionally, an occasional type I burst from 4U 1728−34 was observed while the PCA was pointed directly at the RB. These bursts were easily distinguished from RB bursts by their peak flux (∼15,000 PCA cts s^{-1}) and characteristic light curves, both of which differ markedly from bursts emitted by the RB. We also detected the well-known 363 Hz oscillations (Strohmayer et al. 1996) from several of the 4U 1728−34 type I bursts.

3 OUTBURST EVOLUTION

With the *RXTE* ASM we can detect the onset of a RB outburst to within less than one day. The four outbursts observed with *RXTE* began on 13 April 1996, 30 October 1996, 25 June 1997, and 28 January 1998. The intervals between the start of these outbursts are 200, 238, and 217 days, respectively. Using these three values, we find the current average recurrence time for RB outbursts to be 218 days.

The four most recent outbursts have all followed a nearly identical evolution in the ASM (Figure 2). The time-averaged X-ray flux (PE and bursts) observed with the ASM rises linearly at the beginning of an outburst and peaks within ∼1–3 days. The average X-ray flux then declines exponentially over the next ∼35 days. During the May 1996 and January/February 1998 outbursts, there are indications of reflares. In both cases, in addition to the main peak, two additional peaks are preferred, as determined by F-tests (F-

Table 2. Parameters describing the best-fit curve of each Rapid Burster outburst. The outburst rise is linear, while during outburst decay the ASM flux $\propto e^{-t/\tau}$. The times of the additional peaks (modeled as Gaussians) are given in days since the primary peak. We do not identify any additional peaks during the November 1996 or June/July 1997 outbursts.

					Additional Peaks		
Outburst	Start Time (t_o, MJD)	Rise Time ($t_p - t_o$, days)	Peak Flux (P, ASM cts s^{-1})	τ (days)	Centre ($t_n - t_p$, days)	Amplitude (A_n, ASM cts s^{-1})	Width (σ_n, days)
May 1996	50186.2±2.0	2.4±0.04	16±2	7.9±0.5	8±0.5	3.0±0.2	0.5±0.2
"					13±0.5	2.8±0.2	0.5±0.2
Nov 1996	50386.0±1.2	1.9±0.03	26±2	8.6±0.7	–	–	–
Jun 1997	50624.1±1.5	1.7±0.16	26±2	8.5±0.8	–	–	–
Jan 1998	50841.4±1.4	3.1±0.06	21±2	6.0±0.7	17±1.0	5.7±0.5	3.3±0.7
"					23±0.5	1.6±0.6	0.4±0.3

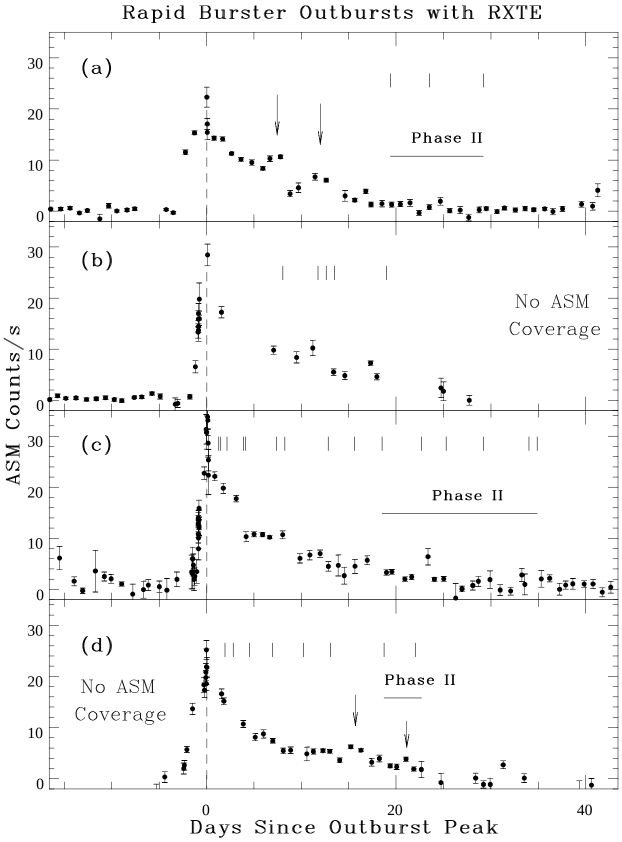

Figure 2. One-day averages of ASM count rates for outbursts of the Rapid Burster (90 second data points are also plotted during the outburst rise). The peaks of the outbursts have been aligned. The data are from (a) 29 March 1996 – 27 May 1996 (outburst peak: 14 Apr 96). (b) 15 October 1996 – 18 November 1996 (outburst peak: 31 Oct 96). (c) 10 June 1997 – 8 August 1997 (outburst peak: 26 Jun 97). (d) 25 January 1998 – 13 March 1998 (outburst peak: 30 Jan 98). Short vertical lines indicate days when PCA observations were made. Horizontal lines indicate periods in which the RB was observed to be in Phase II (type II burst dominated); during other periods the RB was in Phase I (type I burst dominated). Arrows point to the fitted centre of a Gaussian curve which may indicate the presence of a reflare (see text). Prior to the start of an outburst, the RB flux detected with the ASM is consistent with zero.

test probabilities with two additional peaks are 99.8 per cent and 99.3 per cent, respectively). There is no evidence for additional peaks during the November 1996 or June/July 1997 outbursts. These reflares are reminiscent of the behavior of soft X-ray transients (Augusteijn, Kuulkers, & Shaham 1993; for a review of soft X-ray transients, see Tanaka & Lewin 1995). During a one-day period between days 5 and 6 of the June/July 1997 outburst (June 29 and June 30, 1997), there is a sudden decrease in the average flux from the source (see Figure 2c).

An outburst can be parameterized by:

$$f(t) = \begin{cases} \frac{P}{t_p - t_o}\,(t - t_o), & t_o < t \le t_p \\ P e^{-(t-t_p)/\tau} + \sum_n A_n \exp[-\frac{(t-t_n)^2}{2\sigma_n^2}], & t > t_p \end{cases}$$

Here, P is the peak flux (ASM cts s^{-1}), t_o is the time of the outburst start (days), t_p is the time of outburst peak (days), and n parameterizes the additional peaks, with A_n the amplitude of the nth additional peak (in ASM cts s^{-1}), t_n its peak time (days), and σ_n its Gaussian width. The fitted parameters for each outburst are summarized in Table 2.

Our PCA observations of the RB occurred intermittently during four outbursts. The source was observed at varying intervals during each outburst. All four sets of observations, however, are consistent with one global evolutionary pattern for a RB outburst. A RB outburst can be divided into two phases: Phase I is dominated by type I bursts with a strong PE, lasting for 15–20 days. The PE declines steadily during this phase. Phase II consists of several different modes of type II bursting, and lasts until the end of the outburst. Table 3 summarizes the evolution of the RB outbursts.

3.1 Phase I

Within the first 1–3 days of a RB outburst, the persistent emission level rises quickly to its peak level of ~5000 PCA cts s^{-1} (1 count s^{-1} $\simeq 3\times10^{-12}$ erg cm^{-2} s^{-1}, 2–20 keV). Although there have been no PCA observations in this initial rising phase, there have been a few observations near the peak of an outburst. The PE level does not remain constant for any appreciable amount of time; it declines steadily during Phase I from its peak level down to ~1000 cts s^{-1} by the end of the phase.

We observed Phase I to last for 15–20 days. The bursts during this phase that could be positively identified were exclusively type I bursts. The RB type I bursts have a profile

Table 3. The evolution of Rapid Burster outbursts observed by *RXTE* (1 PCA count $s^{-1} \simeq 3\times10^{-12}$ erg cm^{-2} s^{-1}; 2–20 keV).

Days of Outburst	Phase	PE Level (PCA cts s^{-1})	Burst Behavior
1–17	I	$5000 \rightarrow 1000$	Type I bursts 200–250 s duration 1500–3000 s between bursts Possible type II bursts
18–19	II Mode 0	$1000 \rightarrow 700$	Type II bursts long, flat-topped bursts 100–700 s duration Occasional type I bursts
20–21	II Mode I	200–500	Type II Bursts 8–40 rapid bursts (8–12 s duration), followed by a large burst (20–30 s duration) "ringing" during burst decay Small type I bursts may follow large type II bursts
22–35	II Mode II	200–500	Type II Bursts burst intervals can be very regular 40–100 s between bursts burst durations can vary from 5–25 s "ringing" during burst decay Occasional small type I bursts

similar to type I bursts observed from some other LMXBs (Figures 3a & 3b). Typical burst durations were 200–250 seconds, with ∼1500–3000 seconds between bursts. We observed peak excess count rates for these bursts to be typically 2000–5000 cts s^{-1}. The rise times for the bursts decrease as Phase I progresses. Initially, the rise times were 10–20 seconds; however, by day 3 of the outburst the rise times had decreased to 3–5 seconds.

The spectra of 33 out of 35 bursts observed during this phase soften during the burst decay, indicating that they are type I bursts (Figures 4a & 4b). Two bursts did not show detectable spectral softening, and are therefore difficult to classify as either type I or type II (Figure 5). These bursts occurred on day 2 of the June/July 1997 outburst (June 26, 1997), when the PE was at its highest level observed with the PCA (∼5000 cts s^{-1}); moreover, both bursts had peak excess count rates of < 1500 PCA cts s^{-1}. It is possible that these were type II bursts. However, given that these two bursts resemble the other bursts observed during the early stages of Phase I, we feel that they are most likely type I bursts.

3.2 Phase II

We consider Phase II, which is dominated by type II bursts, to begin with the first type II burst. Phase II can be generally divided into three sub-phases, each having a different pattern of type II bursts. Although the start of type II bursting indicates the beginning of Phase II, type I bursting does not cease. Type I bursts identical to those from the first phase can be seen during the initial stages of Phase II. In addition, short type I bursts can be observed throughout Phase II. Although we will describe these sub-phases in the sequence that we observed them to occur, it is important to note that historically the RB has not always followed the same sequence (see Section 4).

On day 18 of the June/July outburst, the RB produced two long, flat-topped type II bursts. These bursts had durations of 180 seconds and >420 seconds (this burst was observed in progress as the spacecraft slewed onto the source). There was very little spectral evolution during the bursts (Figure 3c). Dips were present in the PE following both of the bursts, although there was no dip prior to the only complete burst we observed in this phase. In the last 30 seconds of the shorter burst, the familiar "ringing" of RB type II bursts was evident (Figure 3c). This "ringing" during burst decay is only clearly evident if the bursts are less than ∼200 seconds in duration (Tan et al. 1991). This pattern of flat-topped type II bursts was first observed with *Hakucho* in August 1979, and was called "Phase II" by Kunieda et al. (1984a). This should not be confused with our use of Phase I and Phase II, which describe phases of type I burst-dominated and type II burst-dominated emission, respectively. We propose instead to designate this mode (type II bursts >100 seconds) as "Mode 0", to indicate the fact that it appears to be the initial mode of Phase II. On July 13, 1997, a type I burst was observed while the RB was in Mode 0.

The next burst pattern is characterized by several (8-40) short type II bursts, followed by a larger type II burst (Figures 6a & 6b). Following Marshall et al. (1979), we refer to this as "Mode I". We observed the RB emission in this pattern on February 16, 1998, which was day 20 of that outburst. There was a long delay following each of the large type II bursts before the occurrence of the next type II burst. The shorter bursts had durations of 8–12 seconds, with ∼10 seconds between bursts, while the longer bursts lasted for

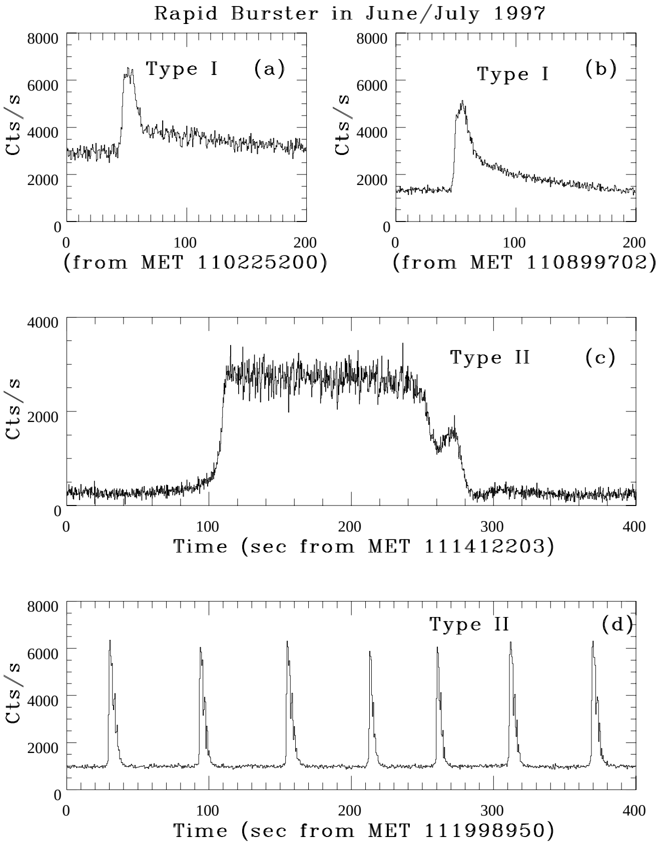

Figure 3. The Rapid Burster during the outburst of June/July 1997. (a) & (b) Type I bursts during Phase I (days 5 & 13 of the outburst). Notice the long tails during the burst decay. (c) Long type II burst during Mode 0 of Phase II (day 19 of the outburst; notice the dip in the PE following the burst). (d) Type II bursts during Mode II of Phase II (day 23 of the outburst). Contributions from 4U 1728-34 have been removed. Figure (b) has been corrected for aspect; this was necessary as that burst occurred during an offset pointing (see text).

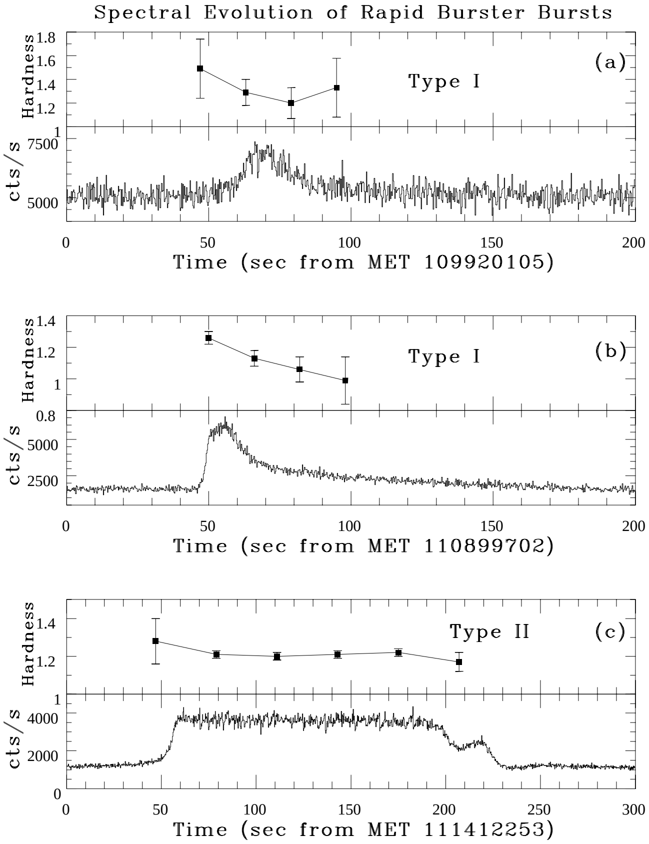

Figure 4. Spectral evolution of Rapid Burster bursts. Hardness is a measure of the blackbody temperature of the excess burst counts above persistent emission. (a) A type I burst that occurred on June 26, 1997 (day 2 of the outburst). When the persistent emission is at such a high level, type I bursts do not always have their characteristic profile. (b) A type I burst that occurred on July 7, 1997 (day 13 of the outburst). Note the drop in the persistent emission level since the burst shown in (a); also note the long tail during the burst decay. (c) A long type II burst that occurred on July 13, 1997 (day 19 of the outburst). Note the lack of spectral evolution and the shape of the burst, making it unquestionably a type II burst (see Tan et al. 1991).

20–30 seconds. The pause following a large type II burst varied from 50 to 350 seconds. There was also a period of enhanced X-ray emission following the large type II bursts. All of the type II bursts observed during this phase exhibited the timescale-invariant profile. Type I bursts can also occur in this phase, usually during the PE period immediately following a large type II burst. This mode is the one observed when the RB was discovered by Lewin et al. (1976).

The final pattern is made up of many short type II bursts in a nearly regular pattern (Figures 3d & 6c), which was designated "Mode II" by Marshall et al. (1979). We observed this mode as the final phase before the end of each outburst seen with *RXTE* (we did not observe the end of the outburst of the RB in November, 1996, since it was too close to the Sun to be observed). The burst profiles are all timescale-invariant, and exhibit "ringing" during burst decay (Tawara et al. 1985; Tan et al. 1991). Burst durations are 5–25 seconds, with bursts occurring every 40–100 seconds. We did observe type I bursts during this phase, some of which occur simultaneously with type II bursts (Figure 6c). At the latest point in an outburst in which we observed Mode II (July 24, 1997; day 30 of the outburst), the burst separation had increased to $\sim$500 seconds.

Mode I and Mode II are distinguishable in Figure 7. The burst energy E has been plotted for each burst at the approximate day of the outburst in which the burst occurred. There is a bi-modal distribution of burst energies during Mode I, while Mode II exhibits a single-peaked distribution.

3.3 E-Δt Relation

Since its discovery, the RB has been known to have a proportional relationship between the fluence of a type II burst and the waiting time to the *next* type II burst (Lewin et al. 1976). In this sense, the RB behaves like a relaxation oscillator. We have calculated the total energy of 398 type II

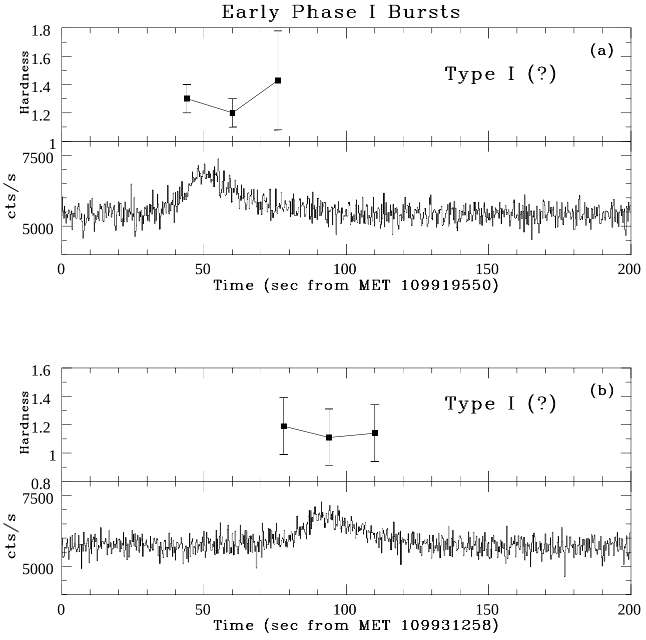

Figure 5. Two bursts from the early stages of Phase I (26 June 1997, day 2 of the outburst). Hardness is a measure of the blackbody temperature of the excess burst counts above persistent emission. The persistent emission level was at its peak during this portion of the outburst. The burst profiles, which are not easily distinguishable as either type I or type II burst profiles, and the poorly constrained spectral evolution make these bursts difficult to classify as type I or type II bursts. Note the slow rise of both bursts.

bursts that occurred during the June 1997 and January 1998 outbursts, assuming isotropic emission and a source distance of 8 kpc. These are plotted against the waiting time to the next burst in Figure 8. In addition, eleven type I bursts from Phase I are included in the figure.

In general, the relationship between the energy in a burst and the waiting time to the next burst can be described by a power law of the form $E{=}\beta(\frac{\Delta t}{100s})^{\alpha}$ (Kunieda et al. 1984a). Here, we have defined β to be the energy in a type II burst that "generates" a 100 second waiting time to the next burst. In rare cases, this E-Δt relation can be approximately linear (α=1). One relation does not hold for all bursts in an outburst, because the time-averaged type II X-ray burst luminosity ($\ell = \frac{E}{\Delta t}$) decreases during an outburst (Figure 2). During our 2–4 ksec observations on any given day, however, α and β remained relatively constant. The derived values of ℓ show a progressive decrease as the outburst evolves. Values for α, β, and ℓ are summarized in Table 4.

The short type II bursts that occurred during Mode I appear to have a nearly constant burst interval, Δt, over a large range of fluences. We do not have enough data points to define a meaningful relation for the bursts that occur at the very end of an outburst (open hexagons of Figure 8). Finally, the E-Δt relation is not relevant for type I bursts (filled triangles of Figure 8).

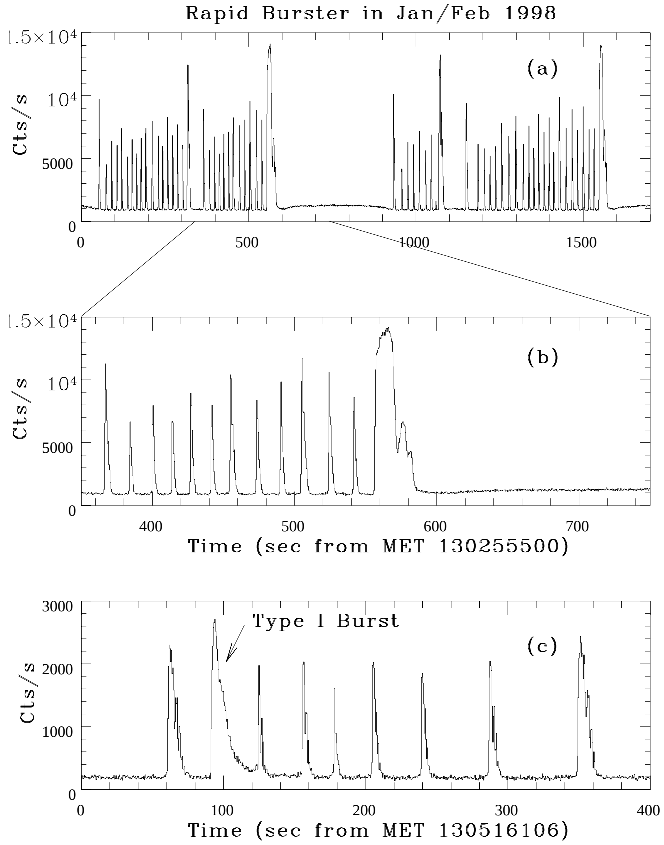

Figure 6. Rapid Burster bursts from the January/February outburst of 1998. (a) Phase II, Mode I (day 20 of the outburst). Note the enhanced emission following the large type II bursts. (b) A 400 second segment of Figure 6(a). (c) Bursts during Phase II, Mode II (day 23 of the outburst). Note the type II burst that occurred during the decay of a type I burst (at time ~100 s). Also note the "ringing" that can be seen during type II burst decay in all three figures.

Table 4. E-Δt relation parameters for type II bursts, where α is the power law index, β is the energy in a type II burst that "generates" a 100 second waiting time to the next burst, and ℓ is the time-averaged type II burst luminosity (see also Figure 8).

Date	Day of Outburst	α	β (10^{39} ergs)	ℓ (10^{37} ergs s^{-1})
16 Feb	20[†]	0.52±0.21	8.5±0.5	8.0±0.2
19 Feb	23	0.94±0.12	3.4±0.2	3.1±0.1
17 Jul	23	0.43±0.13	1.6±0.3	1.7±0.1
20 Jul	26	0.48±0.13	0.53±0.02	1.2±0.1

[†] Only includes the large bursts of Mode I (boxed region of Fig. 7).

4 HISTORICAL PERSPECTIVE

The RB has been observed intermittently since its discovery in 1976 (Figure 1). Various satellites have observed the RB at a variety of wavelengths. X-ray observations of the RB are summarized in Table 5.

Using the 218 day average period determined from the ASM data, we folded the record of RB observations with this

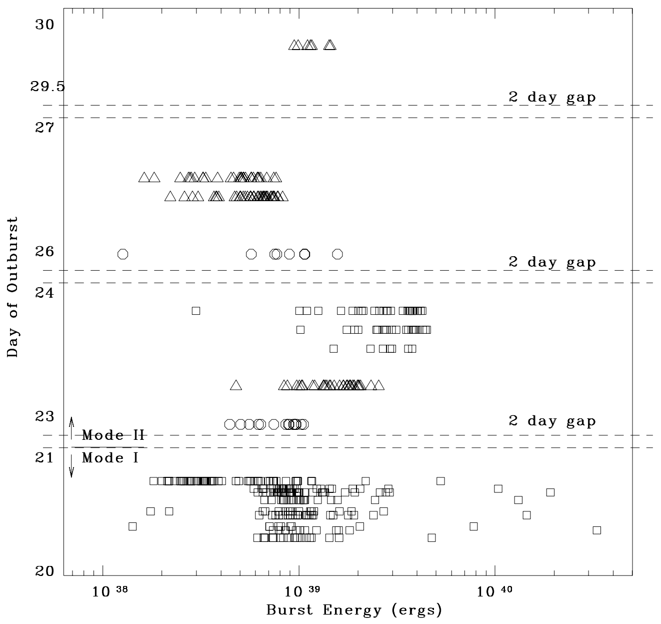

Figure 7. The total energy in all type II bursts observed with *R*XTE. The total energy in each burst (2–20 keV, assuming isotropic emission and a distance of 8 kpc) is plotted against the approximate time of its occurrence. Circles indicate type II bursts of the May 1996 outburst; triangles indicate type II bursts of the June/July 1997 outburst; squares indicate type II bursts of the January/February 1998 outburst. There were no type II bursts observed during the November 1996 outburst. The transition from Mode I to Mode II occurs at approximately day 22 of these outbursts. The results shown in this figure show a striking similarity to those presented by Marshall et al. (1979) in a similar figure. The reader is encouraged to consult the original figure by Marshall et al. (1979).

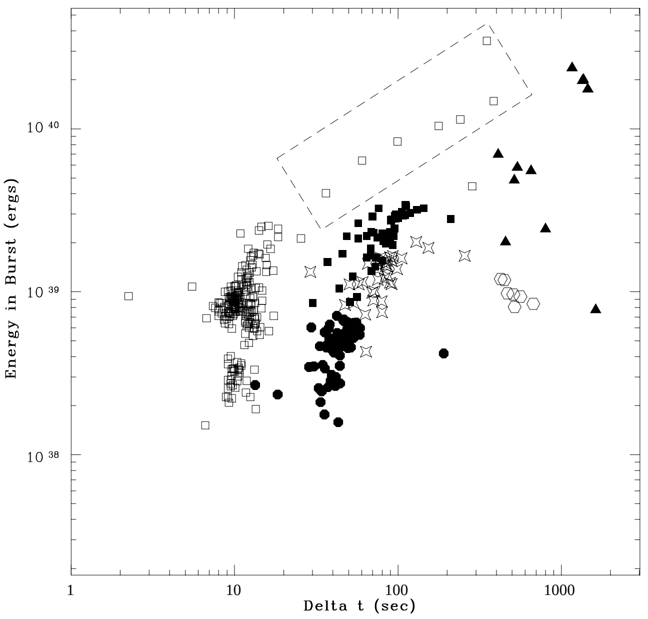

Figure 8. E-Δt Relation. We have assumed isotropic emission and a source distance of 8 kpc. Open squares are type II bursts of Mode I observed during February 1998 (day 20 of the outburst). Those in the boxed region are the large type II bursts of the same mode that were followed by a segment of enhanced PE. Filled squares are type II bursts of Mode II from February 19, 1998 (day 23 of the outburst). Open stars are type II bursts from July 17, 1997 (also day 23 of the outburst; Mode II). Filled circles are type II bursts of Mode II that occurred on July 20, 1997 (day 26 of the outburst). Open hexagons are also type II bursts of Mode II; they occurred on day 29 of the outburst. Filled triangles are type I bursts from Phase I. Note that only bursts occurring on a given day may exhibit a single E-Δt relation, since the time-averaged X-ray luminosity $(\frac{E}{\Delta t})$ decreases during an outburst.

value (Figure 9). The few outbursts that were observed from 1984–1989 seem to fit the pattern reasonably well, while those outbursts prior to 1984 do not fit. In fact, a good fit for the outbursts from 1976–1983 is obtained with a 181 day period. Other periods, from 100–300 days, were also used to fold the data, but none produced better agreement with the observed outbursts than the 181 and 218 day periods. Although years have passed without any positive detections of the RB in outburst, Figure 9 indicates that very few of the observations during those years fell in the estimated outburst windows. It therefore seems likely that the RB goes into outburst at semi-regular intervals of 6–8 months. Continued monitoring with the *RXTE* ASM will be essential to confirm and characterize this behavior.

RB outbursts observed with other satellites have generally followed the evolution that we have described, with some exceptions. In all observations in which the RB was in Phase I (Aug 83, Jun 97, Jan 98), Phase II was observed several days later (Kunieda et al. 1984b). There were two occasions, however, when Phase II may not have been preceded by Phase I. From March 8–15, 1978, *SAS-3* observations indicated that the RB was not in outburst. However, on March 18, 1978, both *SAS-3* and *HEAO I* observed the RB in Phase II (Mode I) (Jernigan et al 1978). *Hakucho* observations from July 31-August 7, 1979, detected no bursts from the RB. On August 8, 1979, rapid repetitive bursts were observed from the RB, indicating that it was in Phase II (Mode II) (Kunieda et al. 1984a). If Phase I occurred in these cases, it must have been extremely short-lived. In all other observations of the RB in outburst, there is a large enough gap (two weeks) between the last pre-outburst observation and the observation of Phase II for Phase I to have occurred "normally". It thus seems that there is a strong indication that the Phase I to Phase II pattern is characteristic of the RB outbursts.

In all RB observations, Phase II has been observed as the final phase of the outburst. There are indications that the RB follows the progression within Phase II that we have described; that is " Mode 0 → Mode I → Mode II". In July 1984, *Tenma* and then *EXOSAT* observed the RB transition from Mode 0 to Mode I to Mode II (Kawai et al. 1990; Lubin et al. 1991). *HEAO I* and *SAS-3* in March 1978, and *Ginga* in August 1988, observed the transition from Mode I to Mode II (Jernigan et al. 1978; Hoffman et al. 1978b; Dotani et al. 1990). Many satellites have observed Mode 0, and later Mode II, without seeing Mode I in between. These include *SAS-3* in March 1979 (Basinska et al. 1980), *Haku-*

Table 5. X-ray observations of Rapid Burster outbursts from 1971–1998. Phase(s) indicates the burst phase(s) observed with each satellite. Mode(s) indicates the mode(s) observed when the RB was in Phase II.

Obs Date	Satellite	Phase(s)	Mode(s)
Mar 71	*Uhuru*	undetermined	
May 72	*Uhuru*	undetermined	
Apr 73	*Copernicus*	undetermined	
Feb 75	*Copernicus*	undetermined	
Mar 76	*SAS-3*	II	I
“	*Ariel V*	II	II → I
Apr 77	*Ariel V*	II	II → I → II
Sep 77	*SAS-3*	II	II
Mar 78	*HEAO I*	II	I
“	*SAS-3*	II	II
Oct 78	*SAS-3*	II	II
Mar 79	*SAS-3*	II	0 → II
“	*Einstein*	II	II
Aug 79	*Hakucho*	II	0 → II
Apr 83	*ASTRON*	I	
Aug 83	*Tenma*	I	
“	*ASTRON*	I	
“	*EXOSAT*	I → II	II
“	*Hakucho*	II	0 → II
Jul 84	*Tenma*	II	0 → I → II
“	*EXOSAT*	II	II
Aug 85	*EXOSAT*	II	0 → II
Aug 88	*Ginga*	II	I → II
Jan 89	*Ginga*	?	
May 96	*RXTE*	II	II
Nov 96	*RXTE*	I	
Jun 97	*RXTE*	I → II	0 → II
Jan 98	*RXTE*	I → II	I → II

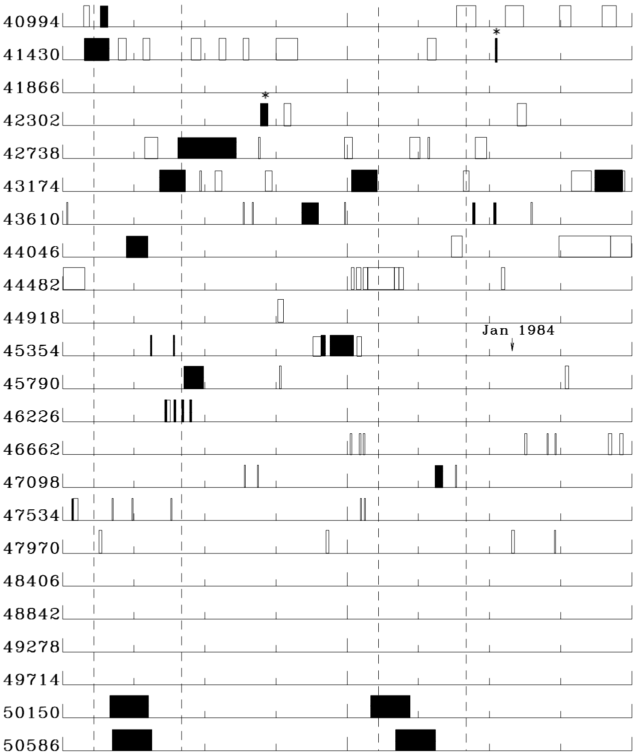

Figure 9. Observations of the Rapid Burster (1971-1998), folded with a 218 day period (2 cycles per line). Modified Julian Dates (MJD) are listed along the ordinate. Filled boxes indicate observations that occurred when the RB was active. Open boxes indicate observations in which the RB was inactive. Single lines indicate observations of less than one day in which the RB was inactive. The observations marked with “*” indicate periods in which the source may have been active, but this is uncertain (White et al., 1978). Dashed lines indicate 65 day windows. MJD 40994 corresponds to February 12, 1971.

cho in August 1979 and in August 1983 (Inoue et al. 1980; Kunieda et al. 1984a; Kunieda et al. 1984b), and *EXOSAT* in August 1985 (Stella et al. 1988a; Lubin et al. 1992b). However, Mode I might have occurred between these observations, since all of the observations were intermittent. All of these observations saw Phase II, Mode II, as the final Mode before the end of the outburst.

Dips in the persistent emission prior to and just following a type II burst are common when the RB is in Mode 0, as is enhanced PE following the large type II bursts of Mode I. This enhanced PE during Mode I can be clearly seen in the first *SAS-3* observation of the RB (Lewin et al. 1976), in the *HEAO I* observation from March 1978 (Hoffman et al. 1978b), and in the *Ginga* observations of August 1988 (Dotani et al., 1990). They are also clearly evident in Mode 0 in observations made by *SAS-3* in March 1979 (Basinska et al. 1980), by *Hakucho* in August 1979 (Kunieda et al. 1984a), and by *EXOSAT* in 1985 (Stella et al., 1988a; Lubin et al., 1993). We observed with *RXTE* a post-burst dip on July 13, 1997 (Mode 0), but no pre-burst dip. However, *Tenma* observed the RB in Mode 0 in August 1983, and did not detect any preceding or following dips in 15 long (>100 seconds) type II bursts (Kunieda et al. 1984b). Of course, instrument sensitivity is an important factor in the detectability of dips in the PE, and *Tenma* may not have been sensitive enough to observe such dips.

There are some exceptions to this evolutionary pattern, however. When the RB was discovered in 1976, Mode I was observed, followed by Mode II. The RB then briefly returned to Mode I before ending in Mode II (Lewin et al. 1976; Ulmer et al. 1977, Marshall et al. 1979). In April of 1977, *Ariel V* and *SAS-3* saw the RB in Mode II, then Mode I, and then finally Mode II again (White et al. 1978, Marshall et al. 1979).

In addition, the duration of the sub-phases of Phase II can vary. We observed Mode 0 and Mode I to last for no more than ∼3 days each. In 1979, however, *Hakucho* observed Mode 0 from August 8–16 (Kunieda et al. 1984a). In 1984, *Tenma* observed Mode 0 from July 2–5, and Mode I from July 6–9 (Tawara et al. 1985).

There are also many idiosyncrasies associated with Phase II. In September 1977, when the RB was in Mode II, a larger than normal type II burst followed a type I burst on four occasions (Hoffman et al. 1978a). This led to the realization that the type I bursts must have come from the RB. Also, Lubin et al. (1993) reported “glitches” that were observed following 10 of 84 long type II bursts observed with *EXOSAT* in August 1985.

5 DISCUSSION AND SUMMARY

In four RB outbursts observed with *RXTE* we have noted a more or less consistent evolutionary pattern that is also reasonably consistent (though not exclusively) with previous observations of the RB. The outbursts begin suddenly and rise to their peak persistent emission (PE) level within three days. Type I bursts dominate for 15–20 days, with a steadily declining level of PE (Phase I). By approximately day 18 of the outbursts, type II bursts appear (Phase II). There are three main types of type II burst patterns: long, flat-topped bursts; a series of short bursts followed by a large burst; and rapid bursts at regular intervals. The rapid, regular bursts are the final phase of any outburst.

During the three outbursts in which Phase II was observed, the phase did not begin until the PE luminosity had decreased to $\sim 2\times10^{37}$ erg s^{-1}. It seems likely that the PE level has important implications for the burst behavior of the RB.

In addition, the fact that type I bursts observed during Mode I occur preferentially during the period of enhanced PE has important implications for the mechanism that triggers type I bursts. Since the periods of enhanced PE always follow a large type II burst, it seems plausible that the thermonuclear flash is triggered by the extra amount of material that has been accreted onto the neutron star.

Using the relation $E=\beta(\frac{\Delta t}{100s})^{\alpha}$ to relate the energy of a type II burst, E, to the waiting time to the next burst, Δt, we find α values in the range 0.43–0.94 for Mode II and the large type II bursts of Mode I. The short type II bursts of Mode I have a relatively constant burst separation, Δt, of $\sim$10 seconds, even though they vary in energy.

The current average recurrence time for RB outbursts is $\sim$218 days. This agrees reasonably well with all observed outbursts after 1983. For outbursts prior to 1984, an average of $\sim$180 days seems more suitable.

The possible reflares that might be present in two out of four outbursts observed with *RXTE* are reminiscent of the echoes observed in some soft X-ray transients. This could be the result of an echo of the main outburst, in which either the companion star or the disk itself is heated by X-rays from the main outburst. The increased mass flow to the accretion disk that results from the heating of the companion star, or the excitation of the accretion disk if the disk itself is heated, could produce a response that we observe as a reflare of X-ray emission (Augusteijn, Kuulkers, & Shaham 1993; Tanaka & Lewin 1995). The delay between the onset of the outburst and the echo, in this model, is related to the time required for matter to be transferred from the location in the disk where the disk instability occurs to the surface of the neutron star.

5.1 Acknowledgments

WHGL gratefully acknowledges support from the National Aeronautics and Space Administration. MK gratefully acknowledges the Visiting Miller Professor Program of the Miller Institute for Basic Research in Science (UCB). We thank the Netherlands Organization for Research in Astronomy ASTRON for financial support.

REFERENCES

Augusteijn T., Kuulkers E., Shaham J., 1993, A&A, 279, L13

Barr P. et al.,1987, A&A, 176, 69

Basinska E. M., Lewin W. H. G., Cominsky J., Van Paradijs J., Marshall F. J., 1980, ApJ, 241, 787

Dotani T. et al., 1990, ApJ, 350, 395

Grindlay J. E., Hertz P., Steiner J. E., Murray S. S., Lightman A. P., 1984, ApJ, 282 L13

Guerriero R. A., Lewin W. H. G., Kommers J., 1997, IAUC No. 6689

Guerriero R. A., Fox D. W., Lewin W. H. G., Rutledge R. E., Moore C., Van der Klis M., Van Paradijs J., 1998, IAUC No. 6815

Hoffman J. A., Marshall H. L., Lewin W. H. G., 1978a, Nat, 271, 630

Hoffman J. et al., 1978b, Nat, 276, 587

Inoue H. et al., 1980, Nat, 283, 358

Jernigan G., McClintock J., Marshall H., Chartres M., Hoffman J., Lewin W., 1978, IAUC No. 3204

Kawai N., Matsuoka M., Inoue H., Ogawara Y., Tanaka Y., Kunieda H., Tawara Y., 1990, PASJ, 42, 115

Kommers J. M., Fox D. W., Lewin W. H. G., Rutledge R. E., Van Paradijs J., Kouveliotou C., 1997, ApJ, 482, L53

Kouveliotou C., Van Paradijs J., Fishman G. J., Briggs M. S., Kommers J. M., Harmon B. A., Meegan C. A., Lewin W. H. G., 1996, Nat, 379, 799

Kunieda H. et al., 1984a, PASJ, 36, 215

Kunieda H. et al., 1984b, PASJ, 36, 807

Lamb P., Sanford P. W., 1979, MNRAS, 188, 555

Levine A., Bradt H., Cui W., Jernigan J., Morgan E., Remillard R., Shirey R., Smith D., 1996, ApJ, 469, L33

Lewin W. H. G. et al., 1976, ApJ, 207, L95

Lewin W. H. G. and Joss P. C., in Lewin W. H. G. and Van den Heuvel E. P. J., eds, Accretion-Driven Stellar X-Ray Sources, 1983, Cambridge University Press, 41

Lewin W. H. G., Van Paradijs J., Taam R. E., 1993, Space Science Review,62, 223

Lewin W. H. G., Van Paradijs J., Taam R. E., in Lewin W. H. G., Van Paradijs J., Van den Heuvel E. P. J., eds, X-Ray Binaries, 1995, Cambridge University Press, 175

Lewin W. H. G., Rutledge R. E., Kommers J. M., Van Paradijs J., Kouveliotou C., 1996a, ApJ, 462, L39

Lewin W. H. G. et al., 1996b, IAUC No. 6506

Lewin W. H. G., Morgan E., Fox D. W., Rutledge R. E., 1996c, IAUC No. 6409

Liller W., 1977, ApJ, 213, L21

Lubin L. M., Stella L., Lewin W. H. G., Tan J., Van Paradijs J., Van der Klis M., Penninx W., 1991, MNRAS, 249, 300

Lubin L. M., Lewin W. H. G., Dotani T., Oosterbroek T., Mitsuda K., Magnier E., Van Paradijs J., Van der Klis M., 1992a, MNRAS, 256, 624

Lubin L. M., Lewin W. H. G., Rutledge R. E., Van Paradijs J., Van der Klis M., Stella L., 1992b, MNRAS, 258, 759

Lubin L. M., Lewin W. H. G., Van Paradijs J., Van der Klis M., 1993, MNRAS, 261, 149

Marshall H. L., Ulmer M. P., Hoffman J. A., Doty J., Lewin W. H. G., 1979, ApJ, 227, 555

Moore C., Rutledge R., Fox D., Guerriero R., Lewin W. H. G., Fender, R., Van der Klis M., Van Paradijs J., in preparation

Ortolani S., Bica E., Barbuy B., 1996, A&A, 306, 134

Rutledge R. E., Lubin L. M., Lewin W. H. G., Vaughan B., Van Paradijs J., Van der Klis M., 1995, MNRAS, 277, 523

Rutledge R. E., Fox D., Lewin W. H. G., Van Paradijs J., 1998, IAUC No. 6813

Stella L., Haberl F., Lewin W. H. G., Parmar A., Van Paradijs J., White N., 1988a, ApJ, 324, 379

Stella L., Haberl F., Lewin W. H. G., Parmar A., Van der Klis

M., Van Paradijs J., 1988b, ApJ, 327, L13

Strohmayer T. E., Zhang W., Swank J., Smale A., Titarchuk L., Day C., 1996, ApJ, 469, L9

Tan J., Lewin W. H. G., Lubin L. M., Van Paradijs J., Penninx W., Van der Klis M., Damen E., Stella L., 1991, MNRAS, 251, 1

Tanaka Y., Lewin W. H. G.,in Lewin W. H. G., Van Paradijs J., Van den Heuvel E. P. J., eds, X-Ray Binaries, 1995, Cambridge University Press, 126

Tawara Y., Hayakawa S., Kunieda H., Makino F., Nagase F., 1982, Nat, 299, 38

Tawara Y., Kawai N., Tanaka Y., Inoue H., Kunieda H., Ogawara Y., 1985, Nat, 318, 545

Ulmer M. P., Lewin W. H. G., Hoffman J. A., Doty J., Marshall H., 1977, ApJ, 214, L11

Van Paradijs J., Lewin W. H. G., 1985, A&A, 157, L10

Van Paradijs J., in Lewin W. H. G., Van Paradijs J., Van den Heuvel E. P. J., eds, X-Ray Binaries, 1995, Cambridge University Press, 536

White N. E., Mason K. O., Carpenter G. F., Skinner G. K., 1978, MNRAS, 184, 1P

Zhang W., Giles A. B., Jahoda K., Soong Y., Swank J. H., Morgan E. H., 1993, Proc. SPIE, 2006, 324